International Journal of Heat and Technology
Vol. 42, No. 5, October, 2024, pp. 1787-1793
Journal homepage: http://iieta.org/journals/ijht

Thermodynamic and Fluid Dynamic Analysis of Clamping Force Variability in High-Strength Bolts Across Temperature Extremes in Northern China

Jinglei Han[1], Peng Jia[2*], Guoping Zhang[1], Changsong Zhao[3]

[1] Project Management Office for the Second Section of the Jinan Fenghuang Road North Extension Project, CCCCSHEC Fourth Engineering Company Ltd., Wuhu 241009, China
[2] Technical Center Department Planning, Jinan Rail Transit Group Co., Ltd., Jinan 250000, China
[3] School of Civil Engineering, Shandong Jiaotong University, Jinan 250357, China

Corresponding Author Email: jiapeng1984@163.com

https://doi.org/10.18280/ijht.420533

Received: 12 May 2024
Revised: 6 September 2024
Accepted: 25 September 2024
Available online: 31 October 2024

Keywords:
high-strength bolt (HSB), clamping force, relaxation, temperature effect, experimental research, northern China

ABSTRACT

This study investigates the thermodynamic and fluid dynamic influences on the clamping force of high-strength bolts (HSBs) within a temperature range of -20°C to 60°C, reflective of the climatic conditions prevalent in northern China. Eight HSB specimens were subjected to focused experimental investigations to quantify the effects of thermal expansion and the dynamics of clamping force relaxation under varying thermal environments. It was determined that initial clamping force relaxation, significantly influenced by thermal dynamics, was completed within seven hours at a controlled temperature of 24°C, with observed losses ranging from 1.01% to 3.44%. Furthermore, a substantial degradation of clamping force was recorded, attributed to a thermal gradient, where losses increased up to 19.02% as temperatures rose from 20°C to 60°C. The findings culminated in the development of a thermofluid model, which effectively estimates clamping force behaviour across the studied temperature spectrum. To mitigate the adverse effects of thermal relaxation, a recommendation was made to increase the standard tightening force by 5%, thereby providing critical guidelines for optimising the mechanical integrity of steel connections under thermal stress. These insights are expected to enhance the understanding of clamping force stability in high-strength bolted joints within extreme thermal environments, contributing to the advancement of structural integrity assessments in engineering applications.

1. INTRODUCTION

HSB connections are pivotal in the assembly of substantial steel infrastructures such as bridges, celebrated for their excellent load-bearing strength, fatigue resistance, and straightforward assembly [1]. The performance and reliability of these connections are critically influenced by environmental temperature fluctuations, necessitating a profound understanding of their thermodynamic and fluid dynamic behaviors.

Firstly, scholars worldwide have focused on the impact of high temperatures on the performance of HSB connections, as HSBs are prone to rapid strength degradation and are among the components most vulnerable to failure under extreme heat. Saglik et al. applied tensile, shear, and combined loads to commonly used grade 8.8 and 10.9 HSBs at temperatures up to 700°C, using numerical simulations to analyze the mechanical performance under these conditions [2]. Mamazizi conducted experimental and simulation-based studies on grade 12.9 and 10.9 HSBs to evaluate their physical properties during fire exposure [3, 4]. Xu et al. [5] investigated the creep relaxation mechanisms in bolt connections without washers under high temperatures. Dai et al. [6] developed a numerical simulation model, defining material constitutive behaviors and contact interactions between assembly components, to analyze bolt forces and deformation at elevated temperatures. Nah et al. [7] proposed methods for estimating bolt clamping force in high-temperature environments. Liu et al. [8] experimentally examined the mechanical properties of HSB connections, focusing on changes in friction coefficient, clamping force, and joint behavior under high temperatures. Additionally, Kumar studied the changes in tensile and shear strength of HSBs after fire exposure and cooling, investigating clamping force loss under different cooling methods and burn conditions [9].

Beyond high-temperature effects, HSBs also experience clamping force loss under ambient conditions. Sakura et al. [10] conducted tests with varying surface pressures and applied forces, developing an equation relating friction coefficient to contact surface pressure. Kong et al. [11, 12] explored the impact of clamping force loss on connection performance at room temperature. Nah and Choi [13] studied clamping force loss across different temperature conditions, focusing on the 10°C-50°C range and developing a regression model for these variations. Data acquisition technology for clamping force is also essential: Huang et al. employed automated digital image

correlation to monitor clamping force in real-time, estimating its loss [14]. Jiang and Zhang conducted experiments on clamping force relaxation by altering bolt grip length and load direction [15, 16]. Yuan et al. [17] measured changes in clamping force using an ultrasonic error compensation model based on solid coupling. Given the typical temperature range of -20℃ to 60℃ in northern China, focused research is needed to understand how these variations impact HSB clamping force.

Given the extreme temperatures ranging from -20℃ to 60℃ typically experienced in northern China, this research aims to integrate a thermodynamic and fluid dynamic framework with mechanical evaluations to thoroughly understand how temperature-induced changes affect the clamping force in HSBs. By combining detailed experimental assessments with advanced thermofluid modeling, this study offers a comprehensive analytical approach that addresses both the thermal expansion and contraction inherent in variable climatic conditions, essential for the design and maintenance of robust steel structure connections.

2. EXPERIMENT PLAN

Initially, eight test specimens were positioned in a constant temperature setting at 20℃ to replicate the relaxation process of clamping force, and the diminishing trend of clamping force in HSBs post-tightening was examined. Following this, they were subjected to controlled temperature environments within a constant temperature chamber and refrigerator to explore the experimental alterations in HSB clamping force with varying temperatures. The primary experimental procedures encompassed [18]:

(1) Manufacturing BFSs. Along the axis of the grade 10.9 M22 HSB, blind holes with a diameter of 2mm and a depth of 28mm were drilled. After cleaning the blind holes, adhesive was poured in and strain gauges were implanted, followed by welding of wires after the adhesive cured.

(2) Calibrating BFSs. The Nake WAW-1000G microcomputer-controlled hydraulic servo universal testing machine with a capacity of 1000kN was used to tension the bolts. Prior to the formal tensioning of the bolts, pre-loading was conducted three times at 50% of the design clamping force. Subsequently, tensioning forces were applied at 20%, 40%, 60%, 80%, and 100% of the design clamping force in five stages. Simultaneously, strain values of the bolts were measured using a static data acquisition instrument, TDS-530. Finally, a calibration equation was established by linear regression analysis between the tension force of each load-sensing screw and the corresponding strain value. Figure 1 illustrates the fabrication and calibration of the load-sensing screws.

(3) Assembly of test specimens: Each test specimen comprises a circular steel washer and a set of grade 10.9 M22 HSB connections, which include one load-sensing screw, one nut, and two washers. The outer diameter of the steel washer is 60mm, the inner diameter is 23mm, and the thickness is 40mm. Figure 2 illustrates the assembly diagram of the test specimens. According to the Chinese JTG D64-2015 specification, the steel washer has a compressive strength of 270 MPa and a yield strength of 345 MPa. The nominal diameter of the FHSB screw is 22mm, graded at 10.9, with a yield strength exceeding 900 MPa and a tensile strength ranging between 1040 and 1240 MPa. The nut grade is 10H, and the washer grade is HRC-45. Each load-sensing screw is tightened to 1.1 times the design clamping force, equivalent to 209kN. During nut tightening, the clamping force is monitored using the strain values displayed by the TDS-530. Furthermore, strain gauges are positioned with perforations at both ends of the HSBs. The vertical distance from the surface of the bolt head to the center positions of strain gauges on specimens Bolt-1 to Bolt-6 and specimens Nut-1 to Nut-2 is measured.

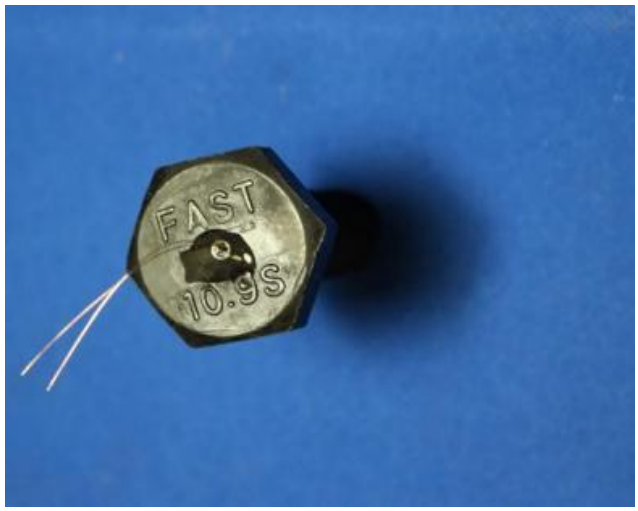

(a) Manufacturing FBS

(b) Calibrating FBS

Figure 1. Production and calibration of the BFSs

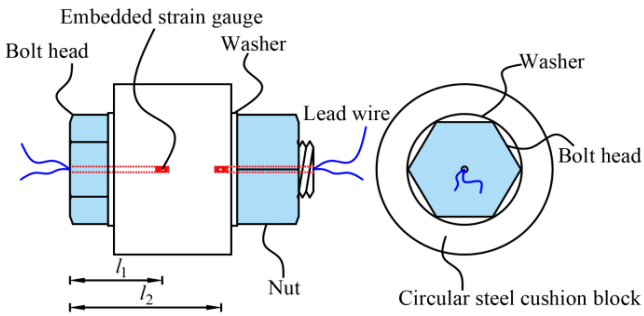

Figure 2. Assembly diagram for the test specimens

(4) Simulation of environmental temperatures: By adjusting the temperature settings of the constant temperature chamber and refrigerator, the variation in clamping force of HSBs was

analyzed across temperatures ranging from -20°C to 60°C. Strain values of HSB specimens were recorded every hour under each temperature gradient, with temperature measurements taken at the same intervals. Additionally, the relaxation of the clamping force of HSBs within 48 hours at an atmospheric temperature of 20°C was investigated. Throughout the experiment, strain values of HSBs and environmental temperatures were logged using static data acquisition instruments and temperature sensors, respectively. Subsequently, environmental temperatures of -20°C, -10°C, 0°C, 20°C, 40°C, and 60°C were simulated using a freezer and oven, with data collected every 24 hours for each temperature gradient. Notably, once a constant temperature is reached, the data acquisition instrument pauses for one hour to allow full thermal conduction within the specimen, after which data collection resumes. Figure 3 illustrates the experimental setup for simulating different environmental temperatures, and Table 1 provides details of the test specimens and relevant parameters.

Table 1. Experimental specimens

Specimen ID	Size	Grade	*l*/mm	Calibration Equation	Correlation Coefficient R^2
Bolt-1	M22	10.9	28	ε=16.32*P*-7.1	0.99
Nut-1			38	ε=16.95*P*-22.9	0.98
Bolt-2			28	ε=15.56*P*-9.2	0.99
Nut-2			38	ε=16.37*P*+8.3	1.00
Bolt-3			28	ε=14.31*P*-28.4	1.00
Bolt-4			28	ε=15.14*P*+8.7	0.99
Bolt-5			28	ε=13.49*P*+12.6	1.00
Bolt-6			28	ε=13.50*P*+12.4	1.00

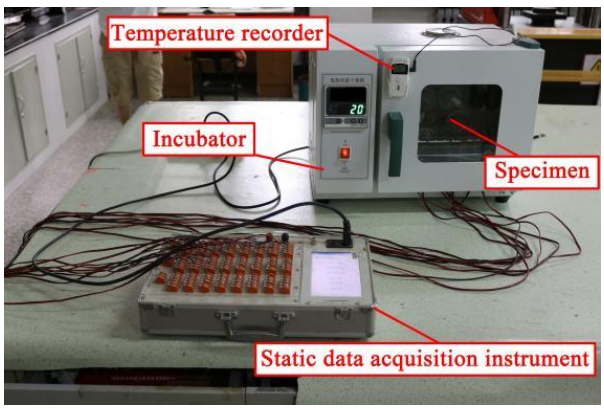

(a) Simulating environmental temperatures at 20°C, 40°C, and 60°C

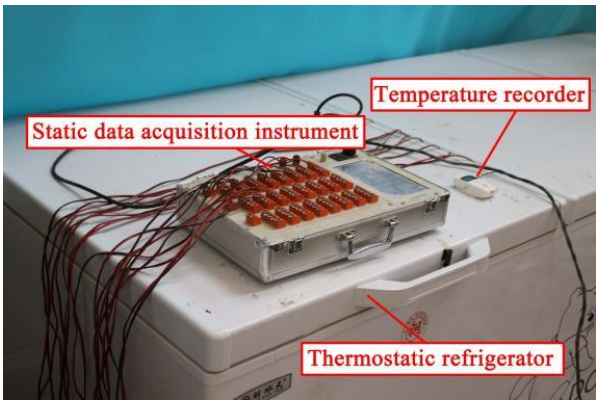

(b) Simulating environmental temperatures at -20°C, -10°C, and 0°C

Figure 3. Experimental setup

3. ANALYSIS OF EXPERIMENTAL FINDINGS

3.1 Relaxation of clamping force

To explore the relaxation behavior of HSBs under a 24°C ambient temperature, the specimens underwent initial pre-tensioning at this temperature. Following this, they were placed in a constant temperature chamber maintained at 24°C. Throughout the experiment, strain values of the HSBs and ambient temperature were monitored using static strain gauges and temperature sensors, respectively, for a duration of 48 hours. Figure 4 depicts the observed variation in clamping force relaxation of HSBs simulated under a 24°C environment over a 48-hour period.

From Figure 4, it is evident that the clamping force relaxation of all specimens follows a consistent pattern over time. Within the initial 5 hours, the clamping force loss peaks, ranging from 1.01% to 3.43%. Subsequently, after 7 hours, the clamping force loss of most specimens stabilizes. After 48 hours, the clamping force loss for all specimens falls within the range of 1.01% to 3.44%. According to the Chinese standard JGJ 82-2011, the final tightening force is prescribed at 1.1 times the design clamping force, with clamping force quality acceptance conducted within 1 hour ≤ t ≤ 48 hours post-final tightening. The experimental findings indicate that the clamping force loss of all specimens is notably below the stipulated 10% in the design. Furthermore, clamping force relaxation is completed within 7 hours. Hence, it is advisable to set the final tightening value at 1.1 times the design clamping force, with clamping force quality acceptance ideally performed within 7 hours ≤ t ≤ 24 hours post-final tightening.

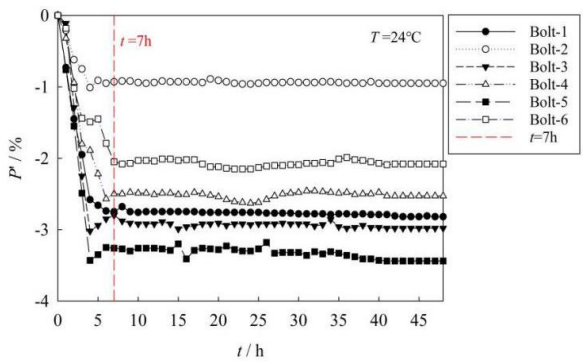

Figure 4. Variation in clamping force relaxation of HSBs in a 24°C environment

3.2 Clamping force temperature effect

Figure 5 illustrates the change in clamping force over time for HSBs under various ambient temperatures. In this figure, the red line represents the temperature gradient over a period of 144 hours, with constant temperatures maintained at -20°C, -10°C, 0°C, 20°C, 40°C, and 60°C for 24 hours each. After the HSB's relaxation at 24°C, the temperature in the constant temperature chamber was sequentially adjusted to 20°C, 40°C, and 60°C. Following each temperature adjustment, strain values for the HSBs were recorded hourly, beginning two hours after the adjustment, with data collection continuing for 24 hours at each temperature. Similarly, the specimen was placed in a refrigerated environment to simulate conditions of -20°C, -10°C, and 0°C, with identical sampling frequency and duration, which will not be reiterated here.

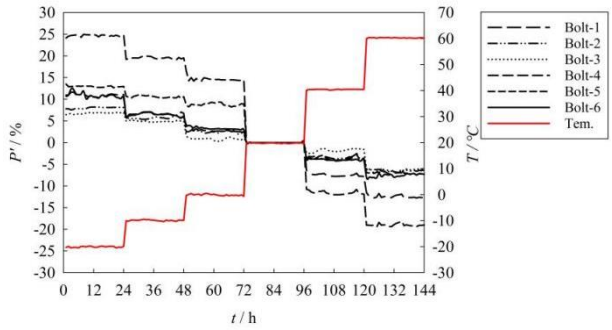

Figure 5. Variation of clamping force of HSBs over time at different environmental temperatures

Table 2 provides a detailed account of the hourly clamping force loss rate for HSBs at constant temperatures of -20℃, -10℃, 0℃, 40℃, and 60℃. Upon completing relaxation at 20℃, the clamping force loss for HSBs at this temperature is defined as zero. The figure reveals that clamping force decreases with increasing temperature and stabilizes at each constant temperature. Additionally, variations in clamping force loss across specimens are observed, attributed to differences in the machining and assembly precision of specimen components.

Table 2. Hourly clamping force loss rate of HSBs under constant temperatures

T/℃	*P′*/%					
	Bolt-1	**Bolt-2**	**Bolt-3**	**Bolt-4**	**Bolt-5**	**Bolt-6**
-20℃	10.96	7.81	6.46	24.13	13.48	10.69
	10.97	7.82	6.56	24.56	12.91	11.03
	11.61	7.53	6.78	24.73	12.96	12.34
	11.69	7.68	6.48	24.77	12.96	12.26
	11.08	7.96	6.58	24.84	13.03	11.25
	11.07	7.84	6.62	24.94	13.04	11.08
	11.34	7.81	6.56	24.29	12.99	11.19
	11.12	7.79	6.80	24.98	13.05	11.88
	10.88	7.84	6.78	24.87	13.07	10.12
	10.52	8.11	6.90	24.86	13.01	10.55
	10.85	8.21	6.96	24.85	13.06	10.84
	10.56	8.19	6.84	24.93	12.89	10.50
	10.54	8.22	6.94	24.77	12.75	10.45
	10.36	8.20	6.84	24.38	12.73	10.26
	10.23	8.15	6.92	24.82	12.74	10.83
	10.69	8.10	6.82	24.84	12.77	10.91
	10.75	8.13	6.86	24.69	13.01	10.58
	11.09	8.10	6.82	24.45	13.05	10.89
	11.23	8.11	6.84	24.69	13.10	11.01
	11.14	8.14	6.86	24.56	12.65	10.92
	11.04	8.13	6.98	24.78	12.93	10.48
	11.01	8.12	6.86	24.58	12.85	10.35
	11.04	8.18	6.89	24.29	12.92	10.19
	11.09	8.10	6.97	24.81	12.98	10.26
-10℃	5.93	5.72	4.98	19.21	10.70	6.19
	6.14	5.64	5.14	19.38	10.48	6.37
	6.28	5.54	5.14	19.50	10.27	6.51
	6.34	5.54	5.12	19.55	10.69	6.55
	6.34	5.57	5.18	19.53	10.84	6.55
	6.34	5.64	4.86	19.49	11.01	6.55
	6.77	5.39	4.88	19.78	10.92	6.87
	6.97	5.37	4.98	19.94	10.85	7.05
	7.00	5.41	4.98	19.95	10.75	7.08
	7.00	5.50	4.72	19.91	10.87	7.08
	6.98	5.58	4.80	19.84	10.69	7.05
	6.54	5.82	4.72	19.52	10.66	6.68
	6.35	5.92	4.80	19.34	10.52	6.49
0℃	6.35	5.93	4.82	19.32	10.40	6.45
	6.47	5.73	4.84	19.47	10.32	6.58
	6.47	5.71	4.86	19.50	10.31	6.57
	6.57	5.56	4.92	19.64	10.36	6.67
	6.58	5.54	4.88	19.67	10.48	6.65
	6.41	5.90	4.86	19.40	10.54	6.48
	6.30	6.10	4.78	19.23	10.34	6.33
	6.25	6.28	5.10	19.06	10.33	6.21
	5.95	6.68	4.80	19.63	10.72	5.91
	5.75	7.06	5.14	19.33	10.05	5.67
	5.95	6.73	4.92	19.55	10.60	5.92
	3.70	2.49	1.47	16.53	8.62	4.11
	3.49	2.54	1.11	14.26	8.25	3.96
	3.26	2.86	0.92	14.97	8.83	3.75
	2.83	2.72	0.85	14.21	8.78	3.40
	3.24	2.64	0.90	14.78	8.59	3.80
	2.83	2.85	0.90	14.13	8.70	3.37
	3.05	2.61	0.85	14.16	8.55	3.49
	2.78	2.09	0.93	14.93	8.93	3.32
	2.82	2.23	0.96	14.86	9.08	3.29
	2.64	2.36	0.89	14.66	9.05	3.15
	2.64	2.53	0.96	14.59	9.31	3.13
	2.62	2.46	0.48	14.59	9.19	3.15
	2.65	2.63	0.30	14.55	9.04	3.19
	2.73	2.10	0.33	14.59	9.37	3.23
	2.57	2.58	0.44	14.46	9.32	3.12
	2.64	2.67	0.56	14.50	8.65	3.17
	2.61	2.82	1.08	14.47	8.60	3.16
	2.61	2.78	1.29	14.49	8.52	3.14
	2.58	2.55	1.25	14.47	8.22	3.13
	2.60	2.77	0.96	14.46	8.43	3.14
	2.56	2.10	0.92	14.40	8.38	3.09
	2.53	1.95	0.68	14.32	8.65	3.06
	2.44	2.26	0.65	14.39	8.98	2.98
	2.41	2.17	1.07	14.38	8.91	2.91
40℃	-6.39	-3.88	-2.4	-10.73	-3.49	-3.79
	-7.02	-3.16	-2.47	-10.94	-3.72	-3.43
	-7.31	-3.27	-2.49	-11.42	-3.83	-3.68
	-7.39	-3.19	-2.38	-11.59	-3.73	-3.77
	-7.38	-3.03	-2.05	-11.53	-3.51	-3.82
	-7.22	-3.73	-1.64	-11.28	-3.13	-3.77
	-7.19	-3.66	-1.42	-11.20	-3.00	-3.80
	-7.09	-3.51	-1.23	-11.06	-2.80	-3.77
	-7.54	-3.26	-1.68	-11.62	-3.65	-4.02
	-7.65	-3.47	-1.84	-11.79	-3.90	-4.04
	-7.72	-3.61	-1.97	-11.90	-4.07	-4.05
	-7.78	-3.73	-2.04	-12.00	-4.20	-4.07
	-7.79	-3.75	-2.07	-12.03	-4.23	-4.06
	-7.74	-3.70	-2.04	-12.00	-4.17	-4.03
	-7.70	-3.63	-1.96	-11.95	-4.09	-4.02
	-7.69	-3.60	-1.82	-11.91	-4.00	-4.04
	-7.70	-3.59	-1.77	-11.90	-3.98	-4.06
	-7.51	-3.28	-1.51	-11.66	-3.61	-3.97
	-7.54	-3.28	-1.43	-11.63	-3.59	-4.01
	-7.38	-2.97	-1.43	-11.40	-3.27	-3.94
	-7.05	-2.29	-1.41	-10.80	-2.52	-3.84
	-7.74	-3.47	-1.42	-11.73	-3.76	-4.13
	-7.75	-3.54	-1.51	-11.80	-3.85	-4.12
	-7.80	-3.63	-1.57	-11.87	-3.93	-4.13
60℃	-11.52	-6.20	-6.22	-19.06	-6.95	-8.06
	-12.34	-6.15	-6.04	-19.06	-7.00	-8.03
	-12.58	-6.28	-6.66	-19.14	-6.93	-8.09
	-12.78	-6.23	-6.89	-19.04	-7.09	-8.05
	-12.57	-6.22	-6.75	-19.62	-6.84	-8.14
	-11.73	-6.14	-6.17	-18.43	-6.80	-7.15
	-12.65	-6.58	-6.09	-19.05	-6.97	-7.85
	-12.41	-6.09	-6.56	-18.97	-6.65	-7.40
	-12.52	-6.30	-6.64	-19.15	-6.93	-7.39
	-12.67	-6.50	-6.68	-19.38	-7.21	-7.45
	-12.69	-6.58	-6.69	-19.41	-7.32	-7.40
	-12.31	-6.96	-6.21	-18.94	-6.67	-7.99

-12.09	-6.99	-6.84	-18.59	-6.90	-7.80
-12.03	-6.93	-6.65	-18.42	-6.83	-7.78
-11.86	-6.96	-6.24	-18.06	-6.63	-7.66
-12.70	-6.15	-6.91	-19.16	-7.04	-7.59
-12.55	-6.34	-6.08	-18.97	-7.03	-7.20
-12.67	-6.48	-6.26	-19.13	-7.29	-7.22
-12.70	-6.55	-6.32	-19.22	-7.38	-7.22
-12.58	-6.40	-6.17	-19.11	-7.18	-7.13
-12.80	-6.61	-6.18	-19.39	-7.48	-7.41
-12.60	-6.39	-6.06	-19.08	-7.16	-7.15
-12.66	-6.44	-6.06	-19.11	-7.24	-7.20
-12.76	-6.31	-6.03	-19.01	-7.11	-7.31

Figure 6 illustrates the regression curve depicting the clamping force loss of HSBs concerning environmental temperature. Within the temperature span of -20℃ to 60℃, specimen Bolt-4 demonstrates the highest clamping force loss at 60℃ environmental temperature, reaching a maximum of -19.02%. At 60℃, the average clamping force loss ratio for all specimens stands at -9.82%. Conversely, at -20℃, the clamping force of all specimens increases, with an average increment of 12.38%. Notably, Bolt-4 exhibits the most substantial increase in clamping force, with a rise of 24.68%. Given that steel bridges in northern China typically undergo temperature fluctuations ranging from -20℃ to 60℃, particularly during hot summers, it is imperative to consider the influence of clamping force loss of HSBs on the joint's slip-bearing capacity.

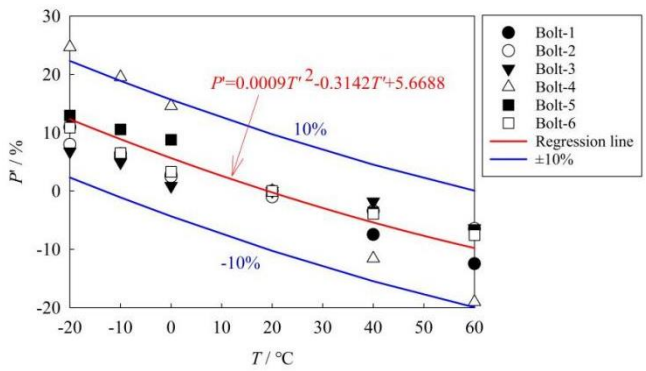

Figure 6. Regression curve depicting the clamping force loss of HSBs relative to environmental temperature

Table 3 presents the average clamping force loss of HSBs for all specimens under the temperature gradient ranging from -20℃ to 60℃. Regression analysis was performed on the clamping force loss data from the six HSB specimens relative to environmental temperature, resulting in the derivation of the regression equation:

$$P' = 0.0009T^2 - 0.3142T + 5.6688 \quad R^2 = 0.7614 \tag{1}$$

In the given formula, T represents the ambient temperature in degrees Celsius (℃); t represents the duration for which the specimen is maintained at a constant temperature of T ℃ (h); P represents the loss ratio of clamping force, equal to $100\% \times (P_T - P_0)/P_0(\%)$. P_0 represents the clamping force of HSBs after relaxation at an ambient temperature of 20℃, while P_T represents the clamping force of HSBs at the ambient temperature T.

Table 3. Average clamping force loss of HSBs at various constant temperatures

Specimen ID	-20℃	-10℃	0℃	20℃	40℃	60℃
Bolt-1	10.95	6.42	2.78	0.00	-7.46	-12.45
Bolt-2	8.01	5.83	2.49	0.00	-3.43	-6.45
Bolt-3	6.79	4.93	0.86	0.00	-1.81	-6.39
Bolt-4	24.68	19.53	14.59	0.00	-11.57	-19.02
Bolt-5	12.96	10.57	8.79	0.00	-3.67	-7.03
Bolt-6	10.87	6.52	3.30	0.00	-3.93	-7.57

Figure 7 displays the influence of temperature on the clamping force of HSBs at different measuring points along the rod axis. The graph illustrates that within the temperature range of -20 to 60℃, the clamping force decreases as the temperature increases for all HSB specimens. Compared to specimens Bolt-1 and Bolt-2, the variations in clamping force between specimens Nut-1 and Nut-2 are relatively minor. Regression analysis of the average clamping force loss at the 38mm measuring point concerning environmental temperature resulted in the following regression equation:

$$P = 0.0012T^2 - 0.2235T + 5.1630 \quad R^2 = 0.9750 \tag{2}$$

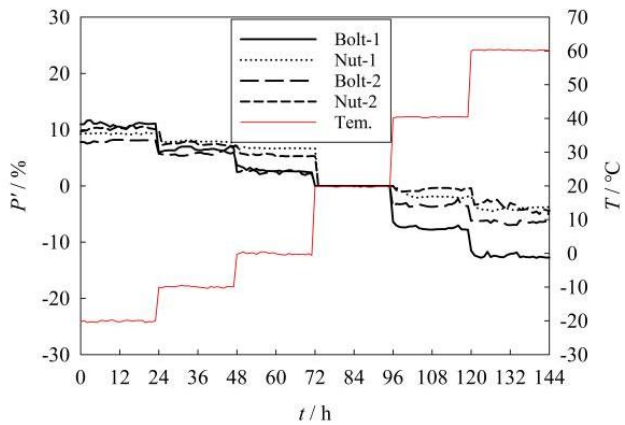

Figure 7. Relationship between clamping force at different positions of HSBs and temperature gradient

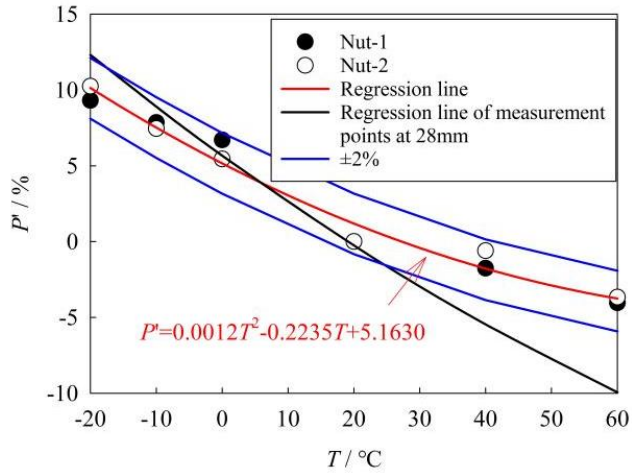

Figure 8. Regression curves of clamping force of HSBs at different measuring point locations with respect to environmental temperature

Figure 8 shows regression curves of clamping force of HSBs at different measuring point locations with respect to environmental temperature. From the graph, it can be observed that there is a notable difference in the regression curve equations of clamping force established at the 28mm and 38mm measuring points under the same environmental temperature. Table 4 provides detailed data on the average clamping force loss of HSBs at the 28mm and 38mm measurement points as a function of ambient temperature. The impact of the measuring point location on the clamping force of HSBs varies consistently with the same temperature, correlating with the complexity of stress along the rod axis. Thus, measuring points should be positioned away from areas of complex stress along the rod axis.

Table 4. Average clamping force loss of HSBs at different temperature gradients and measurement points

Specimen ID	-20℃	-10℃	0℃	20℃	40℃	60℃
Bolt-1	10.95	6.42	2.78	0.00	-7.46	-12.45
Nut-1	9.31	7.85	6.70	0.00	-1.76	-4.04
Bolt-2	8.01	5.83	2.49	0.00	-3.43	-6.45
Nut-2	10.25	7.45	5.45	0.00	-0.60	-3.67

4. CONCLUSION

To examine the clamping force reduction of HSBs at steel bridge joints in northern China, this study simulated the impact of environmental temperatures ranging from -20℃ to 60℃ on the clamping force of these bolts. Experimental investigations were carried out using fabricated test specimens to delve into this phenomenon. The study emphasized the relaxation of clamping force and the effect of temperature gradients on HSB joints in steel bridges in northern China. The primary conclusions derived from this investigation are as follows:

(1) In a 24℃ environment, after tightening the HSB specimens for 7 hours, the clamping force loss essentially reached its peak, ranging from 1.01% to 3.43%. After 48 hours, the clamping force loss ratio for all specimens remained between 1.01% and 3.44%, significantly lower than the 10% stipulated by the Chinese standard JGJ 82-2011. It is recommended that the final tightening of the HSB clamping force is controlled at 105% of the design clamping force. Additionally, quality acceptance of clamping force for HSBs should be conducted 7 hours after final tightening.

(2) Within the temperature range of -20℃ to 60℃, the clamping force of HSBs decreases as the temperature increases. As the environmental temperature rises from 20℃ to 60℃, the maximum clamping force loss of HSBs reaches 19.02%, with an average loss of 9.82%. Since steel bridges in northern China typically experience temperature fluctuations within this range, the impact of temperature on the clamping force of HSBs cannot be ignored. Particularly during hot summers, it is crucial to consider the effect of clamping force loss on the slip resistance capacity of joints in this region.

At different measuring points along the rod axis, the clamping force of HSBs decreases with increasing temperature, and the trend of variation is generally consistent. However, due to the varying complexity of stress at different positions along the rod axis, the sensitivity of clamping force to temperature varies accordingly. Therefore, measuring points should be placed away from areas with complex stress.

REFERENCES

[1] Xu, G.N., Zong, X. (2024). Experimental research on residual clamping force of friction high-strength bolt after corrosion loss simulated by wire cutting. Journal of Bridge Engineering, 29(10): 04024071. https://doi.org/10.1061/JBENF2.BEENG-6642

[2] Saglik, H., Chen, A.R., Ma, R.J. (2024). Ductile fracture of high-strength bolts under combined actions at elevated temperatures. Journal of Constructional Steel Research, 213: 108437. https://doi.org/10.1016/j.jcsr.2023.108437

[3] Mamazizi, A., Ahmadi, A., Khayati, S., Soltanabadi, R. (2023). Experimental study on post-fire mechanical properties of Grade 12.9 high-strength bolts. Construction and Building Materials, 383: 131236. https://doi.org/10.1016/j.conbuildmat.2023.131236

[4] Pang, X.P., Hu, Y., Tang, S.L., Xiang, Z., Wu, G., Xu, T., Wang, X.Q. (2019). Physical properties of high-strength bolt materials at elevated temperatures. Results in Physics, 13: 102156. https://doi.org/10.1016/j.rinp.2019.102156

[5] Xu, H., Wang, W., Ma, Y., Liu, X.W., Xu, X.D. (2013). Analysis of high temperature creep relaxation of bolted joint. Lubrication Engineering, 38(7): 57-60, 79.

[6] Dai, Z.C., Wang, C.Z., Zhou, L. (2016). Finite element simulation preload relaxation of high strength bolt at high temperature. Tool Engineering, 50(5): 41-44.

[7] Nah, H.S., Lee, H.J., Kim, K.S., Kim, J.H., Kim, W.B. (2009). Method for estimating the clamping force of high strength bolts subjected to temperature variation. International Journal of Steel Structures, 9(2): 123-130. https://doi.org/10.1007/BF03249487

[8] Liu, H.B., Liu, D.Y., Chen, Z.H., Yu, Y.J. (2017). Post-fire residual slip resistance and shear capacity of high-strength bolted connection. Journal of Constructional Steel Research, 138: 65-71. https://doi.org/10.1016/j.jcsr.2017.06.026

[9] Kumar, S.M., Darunkumar, K.S., Arul, S.J. (2022). Tensile and shear strength of 10.9 grade bolts in heating and cooling fire. Journal of Constructional Steel Research, 197: 107503. https://doi.org/10.1016/j.jcsr.2022.107503

[10] Sakura, R., Takagi, Y., Hayashi, G., Yamaguchi, T. (2024). Friction coefficient of slip critical bolted joints with inorganic zinc-rich paint focusing on contact surface pressure. International Journal of Steel Structures. https://doi.org/10.1007/s13296-024-00908-6

[11] Kong, Q.Z., Li, Y., Wang, S.Y., Yuan, C., Sang, X.H. (2022). The influence of high-strength bolt preload loss on structural mechanical properties. Engineering Structures, 271. https://doi.org/10.1016/j.engstruct.2022.114955

[12] Kong, Z.Y., Jin, Y., Hong, S.Z., Liu, Q.W., Vu, Q.V., Kim, S.E. (2022). Degradation behavior of the preload force of high-strength bolts after corrosion. Buildings, 12(12): 2122. https://doi.org/10.3390/buildings12122122

[13] Nah, H.S., Choi, S.M. (2008). Estimation on clamping load of high strength bolts considering various environment conditions. Steel and Composite Structures, 24(4): 399-408. https://doi.org/10.12989/scs.2017.24.4.399

[14] Huang, Y.H., Liu, L., Yeung, T.W., Hung, Y.Y. (2008). Real-time monitoring of clamping force of a bolted joint

by use of automatic digital image correlation. Optics and Laser Technology, 41(4): 408-414. https://doi.org/10.1016/j.optlastec.2008.08.010
[15] Jiang, Y.Y., Zhang, M., Lee, C.H. (2003). A study of early stage self-loosening of bolted joints. Journal of Mechanical Design, 125(3): 518-526. https://doi.org/10.1115/1.1586936
[16] Zhang, M., Jiang, Y.Y., Lee, C.H. (2006). An experimental investigation of the effects of clamped length and loading direction on self-loosening of bolted joints. Journal of Pressure Vessel Technology, 128(3): 388-393. https://doi.org/10.1115/1.2217972
[17] Yuan, B., Sun, W., Wang, Y.Q., Zhao, R.X., Mu, X.K., Sun, Q.C. (2023). Study on bolt preload measurement: An error compensation model for ultrasonic detection based on solid coupling. Measurement, 221: 113484. https://doi.org/10.1016/j.measurement.2023.113484
[18] Xu, G.N., Wang, Y.Z., Du, Y.F., Zhao, W.S., Wang, L.Y. (2020). Static strength of friction-type high-strength bolted T-stub connections under shear and compression. Applied Sciences, 10(10): 3600. https://doi.org/10.3390/app10103600